The Experience of DRIVERTIVE-DRIVERless cooperaTIve VEhicle-Team in the 2016 GCDC

Ignacio Parra Alonso, Rubén Izquierdo Gonzalo, Javier Alonso, Álvaro García-Morcillo, David Fernández-Llorca, *Senior Member, IEEE*, and Miguel Ángel Sotelo, *Senior Member, IEEE*

***Abstract*— The second edition of the grand cooperative driving challenge (GCDC2016) was held in The Netherlands in May 2016. Ten international teams participated in the two competition scenarios designed for GCDC2016: platoon merging and intersection. This paper describes the design and development of DRIVERTIVE, a DRIVERless cooperaTIve VEhicle, which aims to advance cooperative automation. The purpose of this paper is to give a general overview of the different designs used to adapt a factory vehicle, with no access to low-level control systems, into a fully-automated cooperative vehicle fit to compete in GCDC2016. The approach taken was pragmatic: different pre-existing techniques for control, state estimation, data fusion, communication, and data degradation were combined and experimentally validated in real-world scenarios, together with other vehicles with different implementations. Our main conclusion is that cooperative autonomous driving is feasible among very different implementations of the communication protocols and using completely different autonomous vehicles.**

***Index Terms*— Cooperative systems, autonomous vehicles, automatization, control.**

I. Introduction and Related Work

AUTONOMOUS driving has become a blooming topic among car makers and research centres all across the globe in the past years since the announcement of Google's self-driving car in 2010. The demonstration of Google's car ability to autonomously drive on highways and urban areas changed many people's minds in the automotive industry, creating a new cohort of what could be coined as self-driving believers. Since then, the interest of car makers in self-driving has not ceased to grow and, as a matter of fact, autonomous driving developments and publications have soared worldwide. Despite rapid technological development, a number of issues, not only legal, have still to be seriously addressed before autonomous cars can robustly, safely, and efficiently circulate and mix with manually-driven vehicles in real traffic. Experts in the field agree that autonomous vehicles will become more robust as they develop further cooperation capabilities. In other words, cooperation with traffic infrastructure, as well as with other vehicles, will make autonomous vehicles more robust and reliable, given that it is widely accepted that standalone self-driving is by far less robust than cooperative automated driving.

The scientific community is clearly moving in this direction. After the first solid demonstrations of self-driving cars in urban scenarios carried out by Google [1], the University of Parma [2], Daimler and KIT on the Bertha Route [3], and a number of other car makers, such as Tesla and Nissan, much research on cooperative automated driving has begun to be developed. Ploeg *et al.* [4] presented a pioneering piece of work in the field of cooperative driving, in which the authors describe the design and development of a Cooperative Adaptive Cruise Control (CACC) system, aiming to increase conventional roads capacity by maintaining a safety time gap between vehicles of less than one second. Their theoretical analysis reveal that this requirement can be met using wireless inter-vehicle communications to provide real-time information of the preceding vehicle, in addition to the information obtained by common Adaptive Cruise Control sensors. Their theoretical hypotheses were validated by means of a series of practical experiments carried out with one test fleet consisting of six passenger vehicles. In May 2011, and coordinated by the same TNO group, the GCDC2011 took place in Helmond [5]. Its objective was to increase the momentum regarding the deployment of cooperative driving, focusing on real-time applications. Nine international teams participated in the challenge. The winning team from KIT [6] implemented a cooperative control strategy divided into two stages. In the first stage, the system calculates an individual acceleration value for each vehicle in the platoon. Each vehicle is considered a single leading vehicle so that the ego-vehicle's optimal acceleration is calculated with respect to such leading vehicle. In a second stage, the controller chooses the minimum acceleration from among all values calculated for each single vehicle. Thus, the resulting cooperative strategy can be considered rather conservative. The Halmstad University team [7] made use of an ACC-equipped production vehicle, which appeared to provide an excellent basis for CACC.

Manuscript received December 9, 2016; revised March 30, 2017 and May 23, 2017; accepted July 10, 2017. This work was supported in part by DGT under Grant SPIP2015-01774 (CUAHC), in part by CAM under Grant S2013/MIT-2713 (SEGVAUTO), in part by the Spanish Ministry of Economy under Grant DPI2014-59276-R, in part by MAPFRE Foundation (MAPFRE-16). This project has received funding from the Electronic Component Systems for European Leadership Joint Undertaking under Grant 737469. This Joint Undertaking receives support from the European Unions Horizon 2020 research and innovation programme and Germany, Austria, Spain, Italy, Latvia, Belgium, Netherlands, Sweden, Finland, Lithuania, Czech Republic, Romania, Norway. The Associate Editor for this paper was E. Semsar-Kazerooni. *(Corresponding author: Ignacio Parra Alonso.)*

The authors are with the Computer Engineering Department, University of Alcalá, 28801 Madrid, Spain (e-mail: ignacio.parra@uah.es).

Color versions of one or more of the figures in this paper are available online at http://ieeexplore.ieee.org.

Digital Object Identifier 10.1109/TITS.2017.2749963

The Chalmers University team [8] contributed by designing and comparing different control strategies (linear and model predictive). The Scoop team [9] participated using one of the largest commercially available road freight lorries. Another heavy-duty lorry was used by the ATeam from Eindhoven Technical University [10], who implemented a two-layered platoon control strategy: a low-level controller to regulate vehicle acceleration and a high-level vehicle-following controller. A similar strategy was applied by the Mekar Team from Istanbul Technical University [11] but implemented it on a compact car instead. More recently, the i-Game research project, funded by the European Commission through the FP7 Programme, organised the GCDC 2016 [12] (Grand Cooperative Driving Challenge 2016) as an innovative and competitive demonstration which took place on the A270 motorway between Helmond and Eindhoven, in the Netherlands. In the 2016 edition of GCDC, 10 European teams competed in a combination of vehicle automation (making it self-driving) and vehicle-to-vehicle (V2V) and vehicle-to-infrastructure (V2I) communication.

A. The 2016 GCDC

The GCDC2016 challenge aimed to *'speed up real-life implementation and interoperability of wireless communication based automated driving'*. Whilst GCDC2011 was oriented towards basic platooning manoeuvres, such as forming and maintaining the platoon, GCDC2016 considered those abilities a prerequisite. The focus of GCDC2016 was on cooperative aspects, with the introduction of advanced platoon operations (merging of two platoons) [13]. To test such cooperative abilities, two scenarios were designed for GCDC2016: highway and intersection.

In the *highway scenario*, two formed platoons in different lanes were required to merge into a predefined competition zone (CZ). The participants were first required to keep the formation at different speeds until the merging was initiated by a message transmited by a Roadside Unit (RSU). Then, a predesigned protocol based on V2V communications between the participants was initiated to achieve the merging of the platoons. This protocol involved the identification of the Most Important Object (MIO) (preceding vehicle) and the two vehicles the ego-vehicle should interact with to perform the merging: the forward MIO (Fwd) and the backward MIO (Back). To dynamically acknowledge these identifications between participants a pairing method based on communications was used prior to the merging maneouvre. A token passing method (the leader flag) was used to allow only one vehicle to merge at a time (the leader). Distance from other participants, gentleness of manoeuvres, reliability of communications and the ability to cope with unexpected situations were evaluated as part of the judging criteria.

In the *intersection scenario*, three vehicles (two competitors and one from the organization) had to manage a T junction spending as little time as possible at the intersection. This scenario started when the two competitors reached a predefined point of the intersection at a given speed in a given time. From that point onwards, the aim was to cross the intersection as fast as possible (30 km/h was the maximum speed), giving way to the organization vehicle and respecting the 'safety distance' in relation to vehicles in the competitors' lane (a 7.5m circumference around every vehicle). As in the previous scenario, the judging criteria were distances, gentleness and reliability. Each scenario was repeated several times (heats) and an average of the best performances was used as final technical score. For further information about the scenarios, please refer to [13] and [14].

B. Outline and Scope

This paper describes the development of DRIVERTIVE, a DRIVER-less cooperaTIve VEhicle which aims to advance cooperative automation, bridging the gap between lab demos and real-life implementation. The purpose of this paper is to give a general overview of the different designs used to adapt a factory vehicle, with no access to low-level control systems, into a fully-automated cooperative vehicle fit to compete in the GCDC2016. The approach taken was pragmatic: different pre-existing techniques for control, state estimation, data fusion, communication and data degradation were combined and experimentally validated in real-world scenarios, together with other vehicles with different implementations.

The remainder of the paper is organised as follows: Section II describes the automatization of the vehicle and low-level controllers for basic control functions. Section III describes the high-level components which facilitate autonomous driving and the state machines which control the complex behaviours in the competition scenarios. Certain results from DRIVERTIVE's participation in the scenarios are also presented and discussed in section IV. Finally sections V, VI and VII analyse DRIVERTIVE's experience from a technical point of view and present possible future lines of research.

II. Vehicle Platform

DRIVERTIVE vehicle is a commercial Citroën C4 with automatic transmission (see Fig. 1) modified for autonomous driving. These modifications involve different hardware components which allow automated control of the steering wheel, accelerator and brake. This section describes the hardware modifications made to the vehicle, the low-level controllers and the system overrides which allow for transition between automated and manual modes. The general architecture of the system is depicted in Fig. 2.

A. Hardware Automatization

In order to have full control of the vehicle, the three main vehicle actuators needed to be automated: the steering wheel, brake and accelerator. In our specific case, only the accelerator was originally controlled by wire forcing us to use mechanical solutions for automation of the steering wheel and brake. These mechanical solutions presented us with challenges which other teams with full by-wire controllable vehicles did not face.

1) Steering Column: A DC motor with a planetary gearhead was connected to the steering column by means of a chain drive. A magnetic clutch is responsible for engagement and disengagement of the DC motor with the chain drive, allowing

Fig. 1. University of Alcalá competition vehicle -DRIVERTIVE-: a modified fuel powered Citroën C4 with automatic transmission.

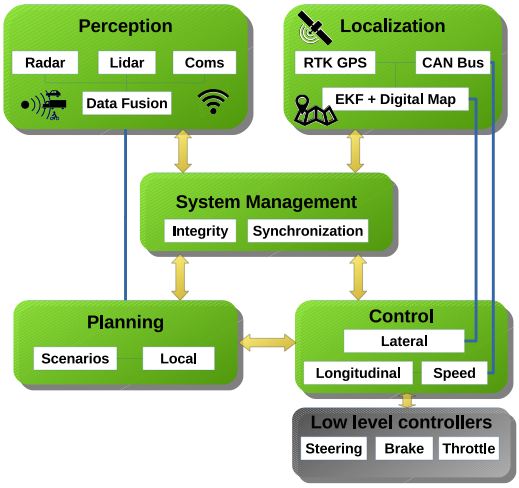

Fig. 2. DRIVERTIVE's system architecture for GCDC2016. The localisation subsystem determines the vehicle's global position with respect to a digital map using positioning information from an RTK GPS and odometry from the vehicle's CAN bus. The longitudinal controller generates acceleration profiles to keep the desired longitudinal distance, the speed controller follows reference speeds from the longitudinal controller. The lateral controller keeps the car centred and aligned in the corresponding lane and performs the turns and lane changes as ordered by the planning subsystem.

us to switch between automatic and manual control. The DC motor is controlled by an Easy-to-use POsitioning System (EPOS) with USB interface which implements a position PID controller.

2) Accelerator: the original by-wire control of the accelerator pedal includes a position sensor mounted on the throttle body. Depending on the opening angle of the accelerator pedal, two different voltage values are applied to the terminals of the vehicle's electronic control module (ECM); V_a and $V_{\frac{a}{2}}$ being $V_{\frac{a}{2}} = V_a/2$. Using a DPDT relay between the accelerator pedal position sensor and the ECM the user can define the operating mode (manual or automatic) by physically connecting to the ECM either the pedal position sensor or the analogue signal from a USB data acquisition module. Using this USB data acquisition module, we can control the accelerator using the following equations to define voltage values:

$$V_a(k) = 0.4 + 3.2 \cdot r(k) \quad (1)$$

$$V_{\frac{a}{2}}(k) = 0.2 + 1.6 \cdot r(k) \quad (2)$$

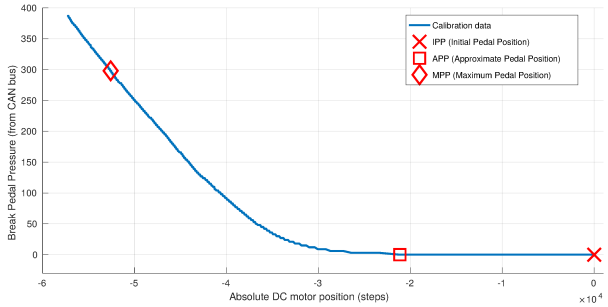

Fig. 3. Pressure over the brake pedal as a function of the DC motor position: calibration data. The negative values correspond to the rotation direction of the motor when winding the wire.

where $r \in [0, 1]$ represents the control reference (0 when released and 1 when fully depressed).

3) Brake: the brake pedal is controlled by means of a mechanical system composed of a DC motor, a planetary gearhead, an incremental encoder, and a wire winding pulley. The DC motor is controlled by means of an EPOS with a USB interface which implements a position PID controller. A wire rope is attached between the pulley and brake pedal. Thus, we can press and release the brake pedal according to the control reference.

The brake pedal pressure (provided by the CAN bus) has a non-linear relationship with the absolute motor position, as can be seen in Fig. 3. To design a controller three different operating points were defined: IPP (Initial Pedal Position), which corresponds to the pedal released; APP (Approximate Pedal Position), which corresponds to the position where no pressure is yet applied to the brake system; MPP (Maximum Pedal Position), which corresponds to the position where maximum pressure is applied to the brake system by a standard driver. Although the system is capable of producing a higher pressure than a human driver, we limited this to ensure the safety of the process. The position of the motor is set to IPP when the longitudinal control is switched off. In order to avoid operation delays, once the longitudinal control is activated, the position of the motor is set to APP. Between APP and MPP points, the desired pressure applied over the brake pedal is given by:

$$P_b = -300 \cdot r(k) \quad (3)$$

where $r(k) \in [-1, 0]$ represents the reference to control pressure over the brake pedal. Once the pressure value P_b is obtained, we use the calibrated non-linear function (Fig. 3) to set the final position of the motor.

B. Low-Level Controllers

1) Steering Wheel Controller: Although the theoretical ratio between motor rotation and steering column rotation can be calculated using torque multiplication and reduction values for the featured components, this ratio will not be accurate due to several factors, such as clearances or clutch slippage. A closed-loop control system was devised to accurately control the steering wheel position. As can be seen in Fig. 4, the reference $r_1(k)$ is the desired steering position in degrees. To close

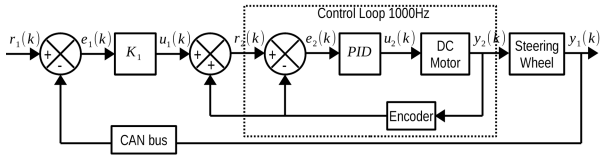

Fig. 4. Low-level closed-loop steering wheel control system.

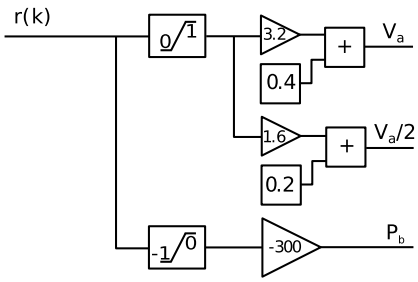

Fig. 5. Accelerator and brake pedal low-level interface.

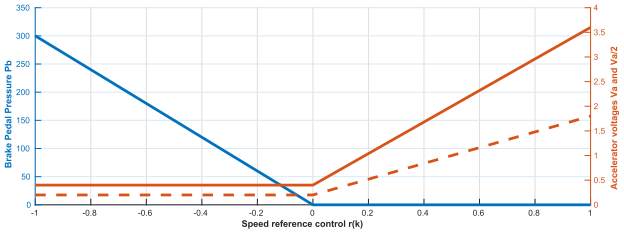

Fig. 6. Accelerator and brake pedal transfer function. In blue brake pedal pressure as a function of the control reference. In red accelerator voltage as a function of the control reference.

the loop, the steering position ($y_1(k)$) was obtained from the vehicle's CAN bus. K_1 represents the theoretical ratio between the steering column and the motor rotations (steps/degrees). Thus, the relative position $u_1(k)$ of the DC motor can be obtained. By adding up the incremental position from the encoder, we can calculate the absolute target position of the DC motor $r_2(k)$. The inner PID control loop runs at 1000Hz whereas the outer control loop runs at 20Hz.

2) Speed Controller: actions over the accelerator and brake pedals must be mutually exclusive. Thus, a unique reference control variable $r(k) \in [-1, 1]$ was defined to set the control action over both pedals, as can be observed in Fig. 5. This interface implements Eqs. (2) and (2) to control the accelerator pedal, as well as Eq. (3) to control the brake pedal. A graphical representation of these control signals is shown in Fig 6. It can be observed that whereas negative values of $r(k)$ involve action over the brake pedal and no action over the accelerator, positive values involve the opposite response. Therefore, the mutually-exclusive response of both actions, accelerating and braking, is achieved.

The low-level speed controller was designed as an Adaptive Proportional (AP) controller, using speed error and current speed as inputs. By introducing an integrator, the system is able to manage acceleration references. However, it is important to highlight that the control is not acceleration-based. The low-level speed controller is shown in Fig. 7.

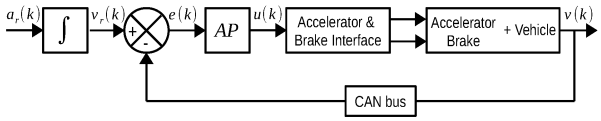

Fig. 7. Adaptive Proportional speed controller.

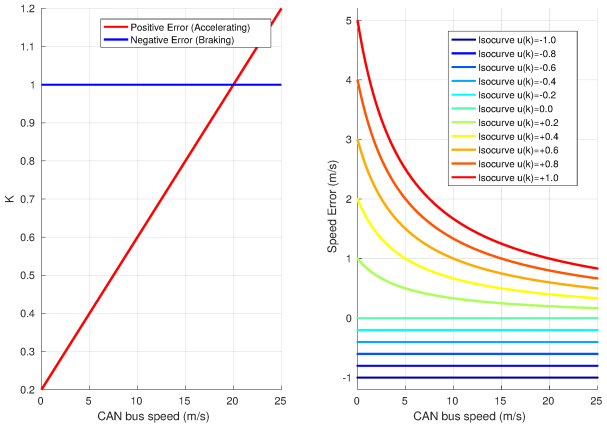

Fig. 8. Left: PA controlller K values as a function of the error (negative means we need to brake, positive to accelerate) and the speed of the vehicle (see Eq. (5)). Right: isocurves for different controller outputs.

The Adaptive-Proportional controller implements the following equations:

$$u(k) = K \cdot e(k) \tag{4}$$

$$K = \begin{cases} K_0 + K_{v0} \cdot v(k) & \text{if } e(k) \geq 0 \\ K_1 + K_{v1} \cdot v(k) & \text{if } e(k) < 0 \end{cases} \tag{5}$$

where K_0 and K_1 correspond to the proportional action when the vehicle is stationary, and K_{v0} and K_{v1} correspond to the adaptive proportional values relating to the vehicle's current speed. Note that when $e(k) \geq 0$ the vehicle must accelerate whereas when $e(k) < 0$ it must brake. Fig. 8 shows the value of K as well as the isocurves for different controller outputs. It can be observed that adaptive acceleration in relation to speed is applied, whereas constant brake action is used. This is mainly due to the fact that braking power depends on vehicle speed, so an adaptive response can be considered an intrinsic feature of the braking process.

To validate the proposed low-level speed controller, a set of experiments were carried out. A trapezoidal speed reference was defined up to 60 km/h. One example of the obtained results is presented in Fig. 9. On the one hand, we can observe that the controller is able to follow the reference shape with a high level of accuracy without overshooting. On the other hand, steady-state error is less than 0.7 km/h for the 60 km/h reference and less than 0.3 km/h for the 30 km/h reference. Note that the controller is not able to remove this error as it is proportional-based.

3) System Overrides: To ensure safety in the GCDC2016 competition, the vehicle's autonomous operation mode should be automatically overridden by a human driver when s/he takes manual control of the steering wheel, accelerator or brake pedals.

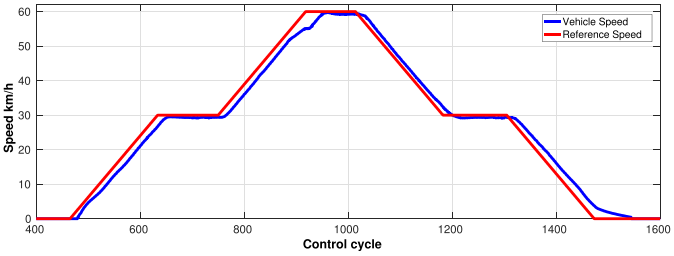

Fig. 9. An example of the adaptive proportional speed controller output using a trapezoidal reference.

a) Steering wheel override: In autonomous mode without human intervention, steady-state error in the steering wheel position is close to zero. When a human driver applies force over the steering wheel, this error increases. In anticipation of this, the steering wheel control system continuously checks for position errors above 5° during at least 500ms (10 control iterations). In this case it is assumed that a human driver is attempting to change the steering and the system is disengaged.

b) Accelerator pedal: The throttle position sensor can be continuously read, even when the relay is connecting our system to the ECM. To detect whether a human driver is pressing the throttle, we check for a voltage greater than 10% of maximum throttle depression. If this is the case, control is returned to the human driver.

c) Brake pedal: To determine whether the human driver is pressing the brake, the pressure over the brake pedal obtained from the CAN bus is evaluated. Two different scenarios may ensue:

- The automated control is accelerating ($r(k) \geq 0$); in this case, the desired pressure over the brake pedal must be zero. Thus, if a human driver applies force over it, the pressure is detected in the CAN bus and the speed control system is disengaged.
- The automated control is braking ($r(k) < 0$); in this case, pressure over the brake pedal will vary between zero and the p_{max}. Thus, it is not possible to detect whether the pressure read from the CAN bus is due to the action of the DC motor or the human driver. However, it was observed that human intervention over the brake pedal caused the vehicle to brake harder than expected by the controller. Thus, in a few control cycles, the vehicle speed dropped below the desired speed and the speed controller attempted to accelerate. As soon as the reference is to accelerate ($r(k) \geq 0$), we find ourselves in the first scenario and the speed control system is disengaged.

In addition to such system overrides, two manual switches on board the cabin must be activated to allow the control signals to pyshically transfer to the actuators (DC motors and electronic signal to the ECM) and can be disengaged at any time, returning control to the human driver.

III. System Architecture

The functional architecture used in DRIVERTIVE autonomous vehicle is based on the five basic functions which drive an autonomous car [15]: perception, localisation, planning, control and system management.

(a) (b)

Fig. 10. Raw RTK GPS trajectory (red) and EKF trajectory (blue). (a) Toll plaza. (b) Under a bridge.

A. Localisation

The localisation subsystem determines the vehicle's global position with respect to a digital map. In order for this to happen, an Extended Kalman Filter first combines the positioning information from the RTK GPS and odometry from the vehicle's CAN bus. Then, the position of the vehicle is matched on a digital map [16] to gather information about its static environment (number of lanes, type of road, orientation, upcoming intersections, speed limits, etc.). The EKF equations were derived from [17], [18], and [19] and adapted to our particular requirements. The state vector $\mathbf{x}$ is composed of easting and northing in UTM coordinates (E, N), vehicle heading φ, speed and acceleration in the heading direction (v, a) and yaw rate $\dot{\varphi}$:

$$\mathbf{x} = \begin{bmatrix} E\,[m] \\ N\,[m] \\ \varphi\,[rad] \\ v\,[m/s] \\ \dot{\varphi}\,[rad/s] \\ a[m/s^2] \end{bmatrix} \tag{6}$$

However, we can only measure our position, speed and yaw rate obtaining an observation vector $\mathbf{z}$ as follows:

$$\mathbf{z} = \begin{bmatrix} E\,[m] \\ N\,[m] \\ v\,[m/s] \\ \dot{\varphi}\,[rad/s] \end{bmatrix} \tag{7}$$

where the yaw rate $\dot{\varphi}$ was calculated from wheels odometry:

$$\dot{\varphi} = \frac{v_r - v_l}{d} \tag{8}$$

being v_r and v_l the right and left rear wheels' respective speeds and d the distance between them.

Our EKF was able to accurately maintain the position of our vehicle with small drifts during GPS blackouts due to the presence of several bridges above the road (see Fig. 10). In addition, DRIVERTIVE was the only team to use a 3G-based virtual correction system [20] which provided us with very accurate RTK corrections during the scenarios. The other teams used a radio-based correction system deployed along the scenarios that suffered from some losts

of coverage. The use of different sources of RTK corrections might account for certain bias observed between most teams' positions and our own. These problems with other teams' positioning, along with loss of communication made it very important to have redundant systems which were able to confirm other participants's positions.

B. Perception

The perception subsystem is responsible for interpreting the information gathered by sensors on board the vehicle and by communications. Its main objective is to maintain an accurate representation of our vehicle's surroundings.

1) Communications: The communications subsystem receives status and environmental information from other vehicles and from infrastructure. The GCDC2016 communications architecture is based on the ITS-G5 V2V standard for V2X communications [21]. This standard uses the GeoNetworking protocol [22] for packet dissemination, the basic transport protocol (BTP) [23] for the transport layer and IEEE 802.11p for the physical layer [24]. This architecture was present in vehicles, as well as in Roadside Units (RSU).

Three different sets of messages were used in the competition: Standard Cooperative Awareness Messages (CAM), Decentralised Environmental Notification Messages (DENM) and the non-standard iGame Cooperative Lane Change Messages (iCLCM). CAM messages contain position, geometry, dynamics and some other optional information whilst DENMs are intended to warn of asynchronous events, such as an emergency vehicle approaching, road-works warnings or the presence of a stationary vehicle. iCLCMs were specifically developed for the competition and were used for the interaction protocols in the different iGame scenarios [14]. Due to the strict safety requirements of the GCDC2016 competition, CAM and DENM messages were broadcasted at 25Hz, more than twice the frequency required by the standard (10Hz). iCLCMs were also broadcasted at 25Hz.

DRIVERTIVE's implementation of its communications system used an ALIX APU1D board running Voyage Linux as its hardware platform. An open-source implementation of Geonetworking [25] along with a customised version of UpperTester was used to connect the vehicle control-computer to the communications box via UDP (see Fig. 11). All of the information transmitted was encoded using ASN.1. Our system decoded these messages using the open source ASN.1 compiler asn1c developed by Lev Walkin [26]. Finally, the UDP package generated by Geonetworking was converted to an Ethernet package using Jan De Jongh's udp2eth [27] and transmitted through the 802.11p wireless interface.

Fig. 12 shows the Complementary Cumulative Distribution Function (CCDF) of CAMs Update Delay (UD) for all teams in heat 1 of the platooning scenario. Each value on the Y-axis represents the probability of receiving two consecutive messages with a delay greater that the value on the X-axis. In contrast to what was expected, some participants showed no stepped CCDF (i.e. 150, 110) but instead much softer distributions. This may indicate that these teams had difficulties generating CAM messages at the required rate, probably due to computational overload. A variable delay in their

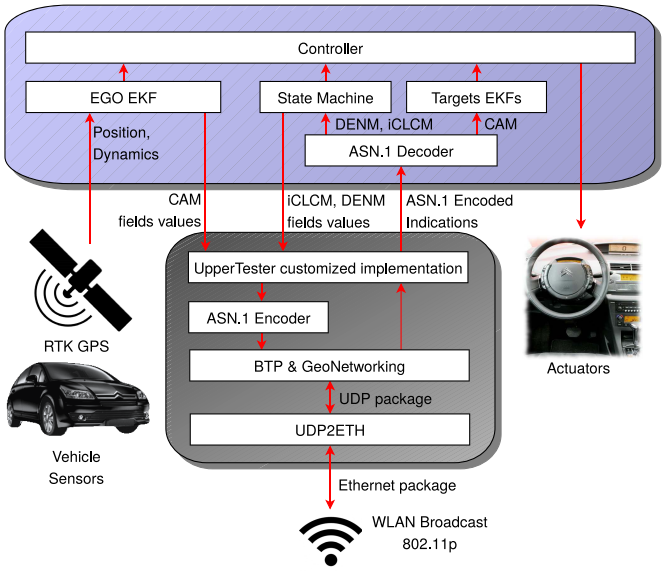

Fig. 11. Communications information flow: the blue box represents the vehicle controller's CPU whereas the black one is the APU1D communications box. Message were exchanged between the vehicle's controller and the communication box using a UDP socket.

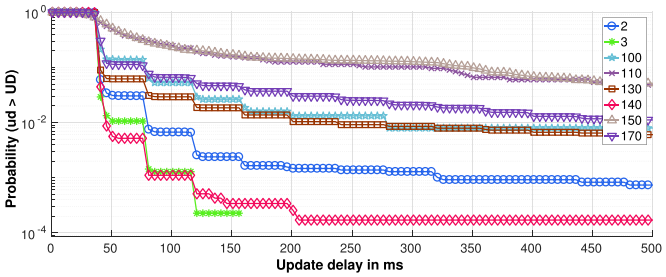

Fig. 12. Complementary Cumulative Distribution Function (CCDF) of CAMs Update Delay (UD) for all competitors in heat 1 of the platooning scenario. Each participant with its ID, is represented with a different color and marker.

systems would cause messages to arrive in a more uniformly-distributed manner. Looking at the other teams, messages from some of them were reliably received and others presented significant UDs. In general, communications were not as reliable as expected, and other sensors were needed to assure the information received through communications. Although further analysis is required, our initial explanation for the communication system's unreliable behaviour is that increasing the broadcasting frequency by a factor of 2.5 and adding a new message (iCLCM) saturated the medium access layer, as observed in [28]. In fact, Decentralized Congestion Control (DCC) mechanism specified by the ETSI recommends to scale the CAM transmission rate to 2Hz in order to not exceed 60-70% of channel load. This has led to proposals such as a mixed CAM transmission system in which smaller CAM messages with critical information are sent at "full" rate (10Hz) and standard CAM messages at 2Hz, reducing the channel load [29].

2) Sensors: DRIVERTIVE is equipped with a four-layer 3D laser scanner SICK LD-MRS40001 embedded on top of the front bumper, a velodyne HDL-32E Lidar mounted

on the roof and a long-range RADAR Continental ARS 300 mounted on the front of the car. For the implementation of GCDC2016 scenarios, we decided not to use both laser scanners.

Therefore, DRIVERTIVE's perception subsystem for the GCDC2016 used only communications and RADAR information to monitor other participants' position, speed, acceleration and heading. Given that communications were not as reliable as expected, Extended Kalman Filters were used to fuse, filter and estimate other participants' state using RADAR and communications information. The implementation of this EKFs was an adaptation of that used to maintain our own state and explained in section III-A.

C. System Management

System management supervises the overall functioning of the vehicle, taking care of the information exchange integrity and the synchronisation between different modules. The CAN bus subsystem, working at 100Hz rate, is used as base time and watchdog for all the other slower subsystems, controlling the update frequency of every other system and time stamping some of the data.

D. Control

The control subsystem follows the commands of the planning subsystem. Whilst the longitudinal controller generates acceleration profiles, the speed controller simply follows reference speeds from the longitudinal controller (see Fig. 2). The lateral controller keeps the car centred and aligned in the corresponding lane and performs the turns and lane changes as ordered by the planning subsystem.

1) Longitudinal Controller: The longitudinal controller was responsible for maintaining an adequate longitudinal distance in relation to other competitors following the commands of the planning subsystem. The distance to be maintained was defined by the GCDC2016 organisers as follows: a fixed safety distance (r) plus a variable distance which depended on the speed of the host vehicle. This variable distance was defined as a constant (headway time t_h) multiplied by the speed of the host vehicle (v_h):

$$d = r + t_h \cdot v_h \tag{9}$$

Assuming constant acceleration for both the host (a_h) and the leader (a_l) the longitudinal controller periodically calculates DRIVERTIVE's required acceleration to be at the required distance and speed (Eq. 9) at a given time horizon (Δt). In short, it calculates the space that the leader vehicle will advance in Δt seconds with its current acceleration a_l and obtains the host acceleration a_h required to meet the conditions in Eq. (9) at time Δt. This acceleration, expressed by Eq. (10), is periodically re-calculated to compensate for both the changes in the leader acceleration and the errors of the speed controller following the references.

$$a_h = \frac{s_l - s_h - r}{\Delta t(th + \Delta t/2)} + \frac{v_l - v_h(1 + \frac{th}{\Delta t})}{th + \Delta t/2} + \frac{a_l \cdot \Delta t}{2th + \Delta t} \tag{10}$$

where s_l and s_h are the leader and host positions and v_l and v_h are the leader and host speeds. The horizon time Δt was experimentally adjusted to be 2s as a compromise between gentleness and time spent to reach the desired distance to the leader. This simple controller, was more stable than more complex ones such as [6] because DRIVERTIVE's unability to follow complex acceleration profiles made them unstable.

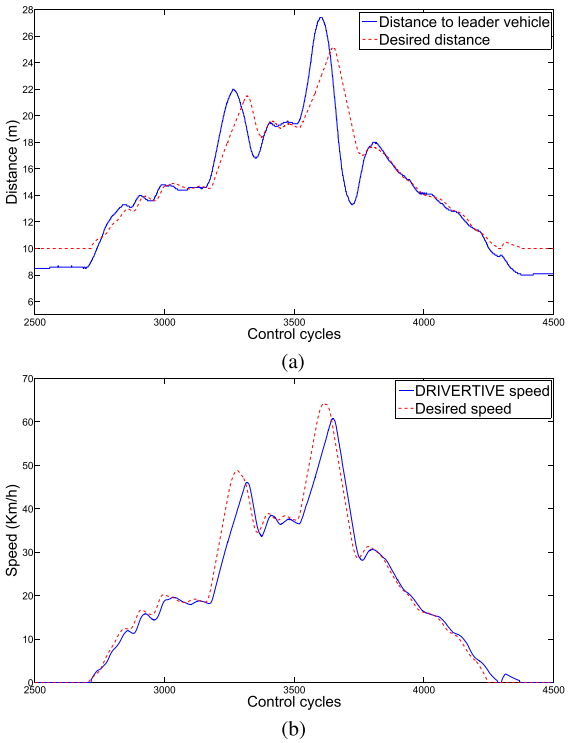

Fig. 13. Results of an experiment following a vehicle with the Longitudinal Controller ($r = 10m$, $t_h = 1s$ and $\Delta t = 2s$). In solid blue are the real distance and speed, in dashed red are the distance and speed requested by the longitudinal controller. (a) Desired distance and distance to leader vehicle. (b) Desired speed and DRIVERTIVE speed.

Fig. 13 shows the results of an experiment in which DRIVERTIVE followed a vehicle using the described Longitudinal Controller with a safety distance (r) of 10 metres, a headway time (t_h) of 1 second and a horizon time (Δt) of 2 seconds. The experiment was divided into three different parts: firstly, the leader vehicle softly accelerated to 20 Km/h. Once that speed was reached, it strongly accelerated first to 40 Km/h, then to 50 Km/h and braked hard, reducing the speed to 30 Km/h. Finally the leader softly decelerated to 0 Km/h. This experiment was designed to explore the controller's response to acceleration and decelerations which DRIVERTIVE cannot reach. Maximum acceleration was limited by software to 2m/s^2 and maximum deceleration to -2m/s^2. In addition, and according to our own calculations, DRIVERTIVE's maximum acceleration was around 1.6-1.8m/s^2, depending on the gear and rpm situation. As can be seen in Fig. 13a when DRIVERTIVE can produce the acceleration, at the beginning and the end, the desired distance is smoothly followed. When DRIVERTIVE is not able to produce those accelerations (see the two peaks in Fig. 13b where DRIVERTIVE's speed falls behind the desired speed) the distance in relation to the leader suffers errors and some overshooting.

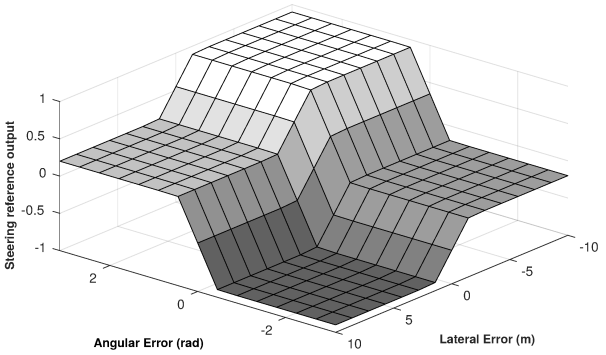

Fig. 14. Output surface of the fuzzy-based lateral controller.

2) Lateral Controller: Due to the non-linear characteristics of a vehicle's movement, conventional control methods require high computational and design efforts. Another approach to lateral control is to use more intuitive techniques based on artificial intelligence that mimic human behaviour and produce *"closer to humans"* styles of driving. Using our previous experience on the design of fuzzy controllers for steering and overtaking maneouvres [30], [31] a fuzzy-logic based controller was developed to perform lateral control. The fuzzy inference motor has two input variables: angular error (the difference in heading between the vehicle and the planned trajectory) and lateral error (the distance between the centre of the vehicle's front bumper and the planned trajectory). The output is the position of the vehicle's steering wheel normalised to the interval $[1, -1]$. The output surface of the fuzzy inference system is shown in Fig. 14.

As can be seen in Fig. 14 this fuzzy controller is proportional, which in practice present some inconveniences. During our tests, the steady state error of the lateral controller was affected by some external conditions such as the wind, the load of the vehicle and the cant of the road. In these cases, the output needed for the vehicle to actually drive straight was different to zero to compensate for the external disturbances. To correct this effect an integrator was added to the reference of the lateral controller that was active only for speeds of 10 Km/h and above:

$$I_k = I_{k-1} + min(0,02, K_i \cdot (r_{lat} - d_{lat})) \tag{11}$$

where I_k and I_{k-1} are the integration values at time k and $k-1$, K_i is the integration constant, r_{lat} is the lateral reference and d_{lat} is the distance to the reference. The integration is limited to 40 cm/s which correspond to the $0,02$ in Eq. (11). The new lateral error is now expressed as:

$$e_{lat} = r_{lat} + I_k - d_{lat} \tag{12}$$

E. Planning

The planning subsystem governs the autonomous vehicle's high-level behaviour based on information from the perception and localisation subsystems and a state machine. Examples of such high-level behaviour are 'change lane', 'keep distance from the car ahead', 'open a gap with the car ahead', 'increase or decrease velocity with a given acceleration', etc. The *local planning* subsystem is responsible for executing this high-level behaviour in a safe and gentle way and takes into account possible unexpected events, such as cars cutting in or pedestrians entering the driving area. In this section, we will explain the implementation of the two GCDC2016 scenarios using different state machines.

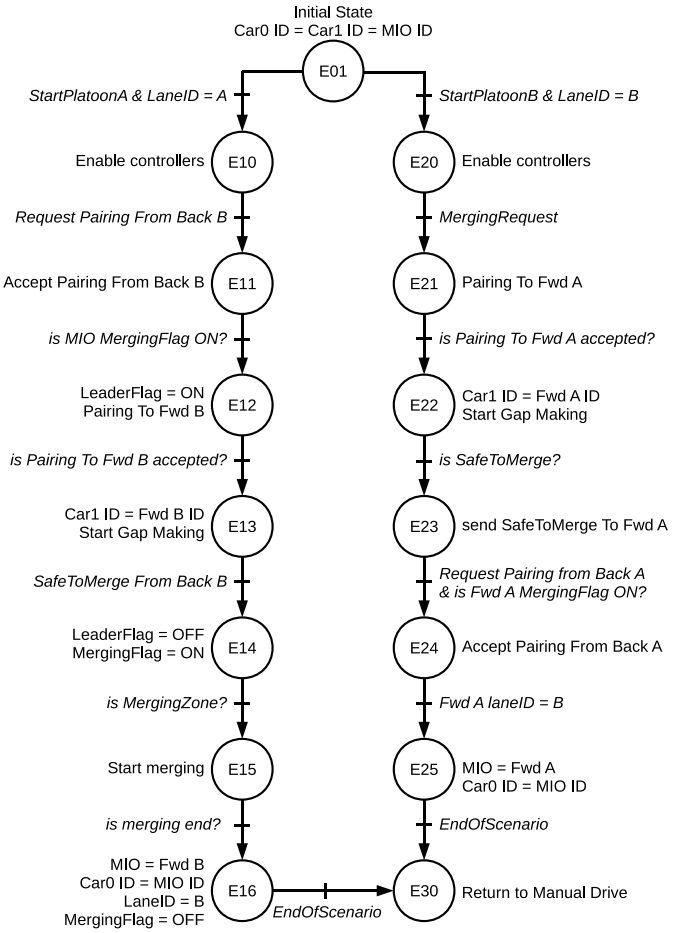

Fig. 15. Flow diagram of the merging scenario. On the left branch when DRIVERTIVE is on the left lane (platoon A), on the right when DRIVERTIVE is on the right lane (platoon B).

IV. Results

A. Merging Scenario

In the merging scenario, platoon A (left lane) needed to merge with platoon B (right lane) as soon as a merging request signal was emitted by a Roadside Unit (RSU). The finite-state machine shown in Fig. 15 was designed to handle all high-level behaviour required to successfully achieve this merging.

Its main tasks were to manage communication exchange with other vehicles, to maintain the platoon, to identify the vehicles which needed to be followed, to open up the required gaps and, finally, to merge if necessary. Some of these tasks were continuously executed (maintaining platoon, managing communications) whilst others were triggered by specific events or situations (opening up gaps or merging). To ensure robust performance throughout the scenario, two cars were tracked at all times. These cars (denoted as Car0ID and Car1ID) changed during the scenario depending on other competitors' situation and position (sometimes Car0ID and Car1ID

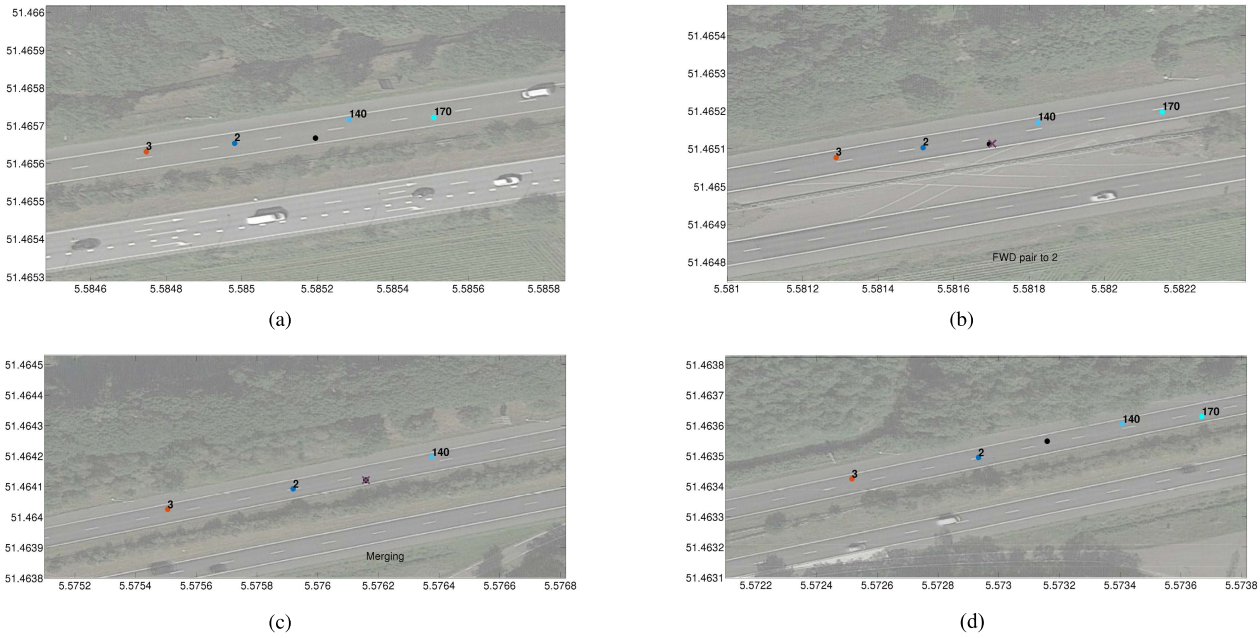

Fig. 16. Representation of the information received through communications for a successful merging manoeuvre from lane A. Platoon A ID's: 3, DRIVERTIVE, 170. Platoon B ID's: 2, 140. DRIVERTIVE's position is represented as a black dot, the remaining teams have their ID overlaid. Important iCLCM messages are represented as Xs. Driving direction is from right to left. (a) Platoon alignment before the pairing. Organization vehicle 3 has already joined platoon B (right lane). (b) After pairing request from 140 (Request pairing from Back B) and acceptation, pairing request to 2 (Pairing to Fwd B) is shown. (c) 140 has opened the gap and sent the Safe TO Merge message (STOM). (d) DRIVERTIVE has sucessfully merged onto platoon B and has passed the leader flag.

could be the same vehicle or on the same platoon, for example when there was only one platoon at the beginning of the heats). Using a conservative approach, Car0ID and Car1ID's position, speed and acceleration were used to calculate our vehicle's desired acceleration, but only the smaller of the two was fed to the controllers.

Fig. 16 shows the sequence of positions received through communications in a merging scenario where DRIVERTIVE successfully merged from lane A. A large X has been used to represent the moment when DRIVERTIVE received or sent some of the important interaction messages (iCLCM). As can be seen, only the immediate surrounding vehicles were received using communications and some of them suffered from frequent losses. The sequence of images shows some of the critical interaction situations which occurred during a merging manoeuvre. Although there is some bias in the GPS positions, vehicles 2 and 140 are on platoon B and 3, DRIVERTIVE and 170 on platoon A. Fig. 16a shows the alignment of the two platoons at the start of the scenario with vehicle 3 already merged on platoon B. Fig. 16b shows pairing request to 2, after pairing request from 140 (Request pairing from Back B) and acceptation. After 140 opened up a gap and sent the Safe TO Merge message, Fig. 16c shows DRIVERTIVE starting the merging after sending the merging message. Finally, Fig. 16d shows the beginning of the merging process for vehicle 170. The performance of the controllers in terms of distance and speed on this scenario are very similar to Fig. 13 which is a much more challenging test for the longitudinal controller as the target vehicle is manually driven.

Despite being able to perform the merging manoeuvres, this scenario presented a serious challenge in terms of DRIVERTIVE system robustness. Three main problems were encountered:

1) *Unreliable Communications:* Communications presented uneven behaviour in terms of reception rate, update delay, range and information reliability. Throughout the heats we were able to consistenly communicate with a few of the teams, had a very short range with others and were practically unable to communicate with others. Because the positions were switched in every platooning heat we faced very different situations and information in every test. In the end we were forced to rely on RADAR information and to use communications only for the interaction protocol (iCLCM) [14].
2) *Unreliable/Unstable GPS Positions:* As can be seen in Fig. 16 the GPS positions transmitted through communications had a significant non-constant drift. DRIVERTIVE was not affected by these drifts on its local navigation/localisation with the exception of loss of GPS coverage under bridges. In these situations the EKF was able to maintain our position, as explained in section III-A.
3) *Non Flexible Interaction Protocols:* While testing the different scenarios in the GCDC, we found that our state machines were too strictly linked to the formal description of the scenarios. In real interactions with the other teams, there was always a message which did not arrive, a distance which was not respected and a position which was not correctly reached, thus blocking the entire

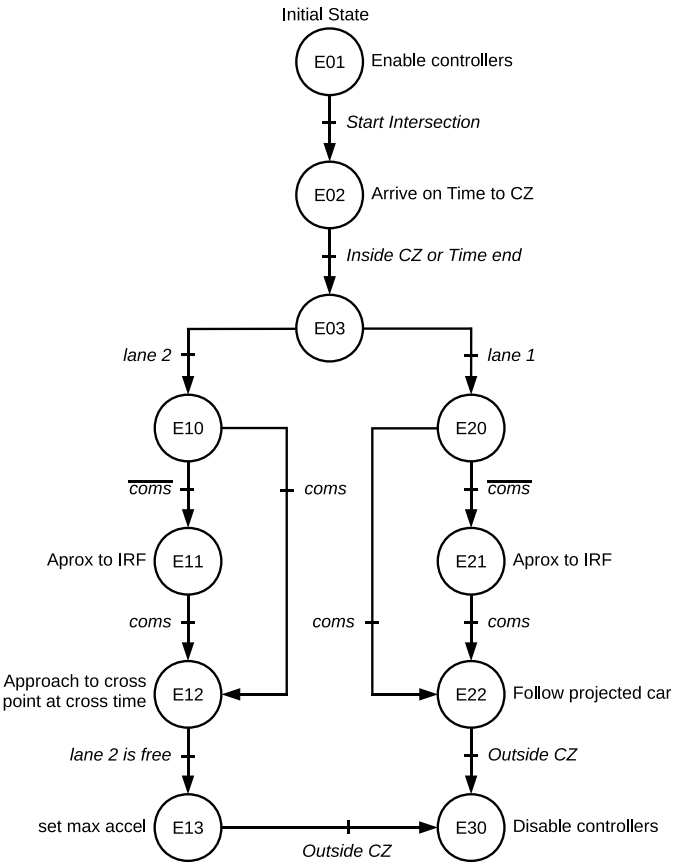

Fig. 17. Flow diagram of the merging scenario. Lane 1 starting from right. Lane 2 starting from left.

protocol execution. After a few tests, it was necessary to add some flexibility and escape routes so as to complete the tests in a consistent manner.

B. Intersection Scenario

In intersection scenario 2 competitors and one organisation vehicle had to manage a T-junction. The organisation vehicle always had priority and competitors were required to cross the intersection in as little time as possible, whilst observing maximum speeds and minimum safety distances between one another. Like in the platooning scenario, a finite-state machine was designed to address all the required high level behaviour (see Fig. 17).

In the intersection scenario, prior to starting the heat, both competitor cars were required to reach the competition zone (CZ), at a given time and fixed speed (30 Km/h). The CZ is a circumference with its centre in the intersection joint point named Intersection Reference Point (IRF) (see Fig. 18). This requirement ensures that all vehicles reach the intersection at the same time and distance.

To enter the CZ at a given time T and given speed v_d DRIVERTIVE implemented an algorithm which continuously adjusts a second-degree polynomial of the necessary acceleration to meet all requirements at time T. This acceleration, speed profile and distance covered (Eq. 13, 14 and 15) define the following system with 5 parameters $[C_0\, C_1\, C_2\, C_3\, C_4]$:

$$a(t) = C_0 t^2 + C_1 t + C_2 \tag{13}$$

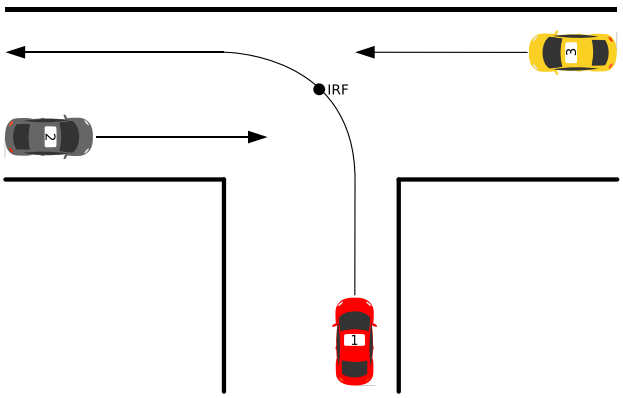

Fig. 18. Representation of the intersection scenario. Cars 2 and 3 are competitors, car 1 is the organisation's. Car 3 is on the right (lane 1). Car 2 is on the left (lane 2)

$$v(t) = \int a(t)\, dt = \frac{1}{3}C_0 t^3 + \frac{1}{2}C_1 t^2 + C_2 t + C_3 \tag{14}$$

$$s(t) = \int v(t)\, dt = \frac{1}{12}C_0 t^4 + \frac{1}{6}C_1 t^3 + \frac{1}{2}C_2 t^2 + C_3 t + C_4 \tag{15}$$

By using five boundary conditions this system can be solved as follows:

1) Initial speed: $v(t=0) = C_3 = V_{t0}$
2) Initial distance (distance to IRF): $s(t=0) = C_4 = S_{t0}$
3) Final acceleration: $a(t=T) = a_d = 0$
4) Final speed: $v(t=T) = v_d = 30$Km/h
5) Final distance: $s(t=T) = r$

After solving the system, the required acceleration can be obtained from Eq. (13) and transformed into speed commands to be transmitted to the low-level controllers. To minimise the effects of errors on the low-level controllers, this acceleration polynomial is periodically recalculated until the CZ is reached.

Once in the CZ, the organization vehicle's position, speed and acceleration is projected onto our lane and the longitudinal controller is requested to follow this projection (using $r = 15m$ and $t_h = 0$ in Eq. (9)). Therefore, DRIVERTIVE gave way to the organisation vehicle until it was in its own lane and then adopted a 'following behaviour'. In the intersection scenario starting from the left, the organisation vehicle simply crossed our lane and the longitudinal controller was requested to follow a car which was at an infinite distance. This caused DRIVERTIVE to accelerate to the maximum permitted speed.

Figs. 19a and 19b show the trajectories and safety distance circumferences for DRIVERTIVE and the organisation vehicle in 2 different intersection heats, one starting from the left and the other from the right. Different markers show both cars' positions at three moments of the heats: circles when DRIVERTIVE entered the CZ, triangles when the organisation enters the intersection (left) or exit DRIVERTIVE's lane (right) and squares when exiting the intersection at the maximum permitted speed. Figs. 19c and 19d show the distances between DRIVERTIVE and the organisation and markers are placed at the same moments as previously. These figures were reconstructed using the communication information transmitted by the organisation vehicle and DRIVERTIVE's communications.

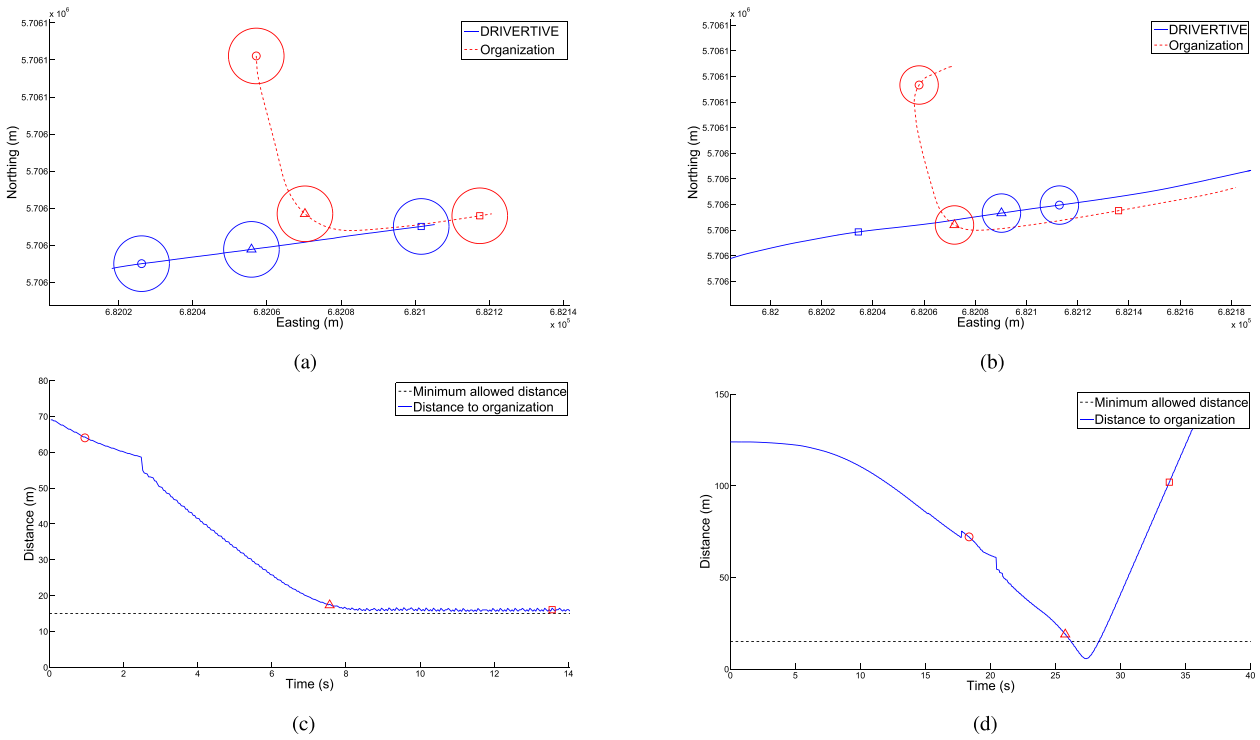

Fig. 19. On the upper row are the trajectories of DRIVERTIVE and the organisation vehicle during 2 intersection heats. On the lower row are the distance between DRIVERTIVE and the organisation vehicle. The markers correspond to different moments of the heat: circles when DRIVERTIVE entered the CZ, triangles when the organisation enters on the intersection (left) or exit DRIVERTIVE's lane (right) and squares when exiting the intersection at the maximum permitted speed. The safety distance for each vehicle is overlaid as a large circle when applicable. (a) Intersection heat trajectories. DRIVERTIVE starts from the right (lane 1). (b) Intersection heat trajectories. DRIVERTIVE starts from the left (lane 2). (c) Distance to organization vehicle received by V2V communications. DRIVERTIVE starts from the right (lane 1). (d) Distance to organization vehicle received by V2V communications. DRIVERTIVE starts from the left (lane 2).

As can be seen in Fig. 19, once DRIVERTIVE entered the CZ it gave way for the organisation vehicle; in reality, the longitudinal controller was requesteded to follow the organisation vehicle's projection onto our lane, so that DRIVERTIVE was approaching an almost-stationary vehicle. Once the organisation vehicle continued in our lane, the longitudinal controller followed the organisation vehicle at the desired distance (see Fig. 19c). When the organisation vehicle simply abandoned our lane (see Fig. 19d), the distance to the vehicle to follow became infinite and the longitudinal controller accelerated to the maximum permitted speed. In the intersection scenario, communications performed unevenly mainly due to signal blockage from a building. However, as the participants got closer to the competition zone (CZ) the messages were received normally (see the distance variations in Figs. 19c and 19d) and the whole intersection scenario could be managed based on communications.

V. Discussion

Despite certain difficulties, during the GCDC2016 it was demonstrated that cooperative autonomous driving was feasible for very different implementations of the standard ITS-G5 and using a tailor-made protocol for the interaction of different vehicles (iCLCM). Generally speaking, DRIVERTIVE's algorithm performance superseded expectations: it obtained the highest technical score and was deemed the 'Best Team with Full Automation'. However, we also experienced countless problems which we addressed to the best of our abilities. In relation to communications we suffered very poor coverage during the preparation week. This was due to our wireless card having two outputs for the antenna pigtail, with one of them presenting a significantly lower performance than the other. Switching the antenna to the second output solved this problem. Regarding hardware automatization we faced more serious issues which eventually led to us failing to finish every competition heat. One of our USB acquisition cards failed on the last day of the competition, leaving our throttle control unusable. Although we cannot be sure of the reasons for this, we can guess that some currents returning from the DC motors to the power supplies were not absorbed; consequently, this caused the EPOS and USB acquisition cards digital logic to fail. Eventually one on them became inoperative. Finally, we discovered that the RADAR produced some false detections when approaching a bridge due to the aperture of the RADAR. Luckily, these candidates were fairly far away and disappeared as we approached the bridges.

VI. Conclusions

DRIVERTIVE team adapted a factory vehicle with no access to the low-level control systems into a fully-automated cooperative vehicle fit to compete in the GCDC2016. As part of this project we:

1) Automated the three main actuators of a factory vehicle so as to fully control the vehicle through a computer.
2) Designed and implemented low-level controllers which allowed us to follow speed profiles and set the steering position from a computer.

3) Designed and implemented the high-level controllers which allowed us to programme trajectories, speed profiles, lane changes, and to follow a vehicle and arrive to a fixed GPS position in a given time and at a given speed.
4) Implemented a communications box, based on the ITS-G5 standard, which is able to interact with other vehicles and with infrastructure.
5) Designed and implemented models and algorithms for state estimation and sensor fusion for the perception subsystem.
6) Designed and implemented two finite-state machines which allowed us to successfully interact with other autonomous vehicles in different situations.
7) Designed and implemented an HMI which allowed us to monitor and control the automated vehicle.

VII. Future Work

DRIVERTIVE learned about numerous aspects of cooperative driving during the GCDC2016 competition, but there are still many open issues which deserve our attention in the future:

- *Reducing the Dependence of the Localisation System on High Accuracy RTK:* Although our localisation system performance was very satisfactory, we understood that for truly autonomous driving, an RTK GPS cannot be the main source of localisation. The price of such systems along with but the need for almost continuous availability of GPS and RTK correction signals, make them an inviable real-world solution. We are currently developing other localisation systems based on feature extraction and map matching to complement non-RTK GPS localisation.
- *Non-Communicating Vehicles:* Although our system was able to deal with non-communicating vehicles, instead of being included in manoeuvres they were simply avoided. In real-world scenarios, non-communicating vehicles would be the majority and would have to be included in high-level planning as more than mere 'obstacles'.
- *Improving Data Fusion:* Our perception system for the GCDC2016 only fused information from communications and the RADAR, thus providing a limited view of our environment. All available sensors should be integrated into the perception system to get a dense 360° representation of our environment.

References

[1] *Google Self-Driving Car Project*. Accessed: Sep. 2017. [Online]. Available: https://www.google.com/selfdrivingcar/

[2] A. Broggi *et al.* "PROUD—Public road urban driverless-car test," *IEEE Trans. Intell. Transp. Syst.*, vol. 16, no. 6, pp. 3508–3519, Dec. 2015.

[3] T. Dang *et al.*, "Making bertha drive—An autonomous journey on a historic route," *IEEE Intell. Transp. Syst. Mag.*, vol. 6, no. 2, pp. 8–20, Summer 2014.

[4] J. Ploeg, B. T. M. Scheepers, E. van Nunen, N. van de Wouw, and H. Nijmeijer, "Design and experimental evaluation of cooperative adaptive cruise control," in *Proc. Int. IEEE Conf. Intell. Transp. Syst.*, vol. 1. Oct. 2011, pp. 260–265.

[5] J. Ploeg, S. Shladover, H. Nijmeijer, and N. van de Wouw, "Introduction to the special issue on the 2011 grand cooperative driving challenge," *IEEE Trans. Intell. Transp. Syst.*, vol. 13, no. 3, pp. 989–993, Sep. 2012.

[6] A. Geiger *et al.*, "Team AnnieWAY's entry to the 2011 grand cooperative driving challenge," *IEEE Intell. Transp. Syst. Mag.*, vol. 13, no. 3, pp. 1008–1017, Sep. 2012.

[7] K. Lidström *et al.*, "A modular cacc system integration and design," *IEEE Intell. Transp. Syst. Mag.*, vol. 13, no. 3, pp. 1050–1061, Sep. 2012.

[8] R. Kianfar *et al.*, "Design and experimental validation of a cooperative driving system in the grand cooperative driving challenge," *IEEE Trans. Intell. Transp. Syst.*, vol. 13, no. 3, pp. 994–1007, Sep. 2012.

[9] J. Mårtensson *et al.*, "The development of a cooperative heavy-duty vehicle for the GCDC 2011: Team scoop," *IEEE Trans. Intell. Transp. Syst.*, vol. 13, no. 3, pp. 1033–1049, Sep. 2012.

[10] M. R. I. Nieuwenhuijze, T. van Keulen, S. Öncü, B. Bonsen, and H. Nijmeijer, "Cooperative driving with a heavy-duty truck in mixed traffic: Experimental results," *IEEE Intell. Transp. Syst. Mag.*, vol. 13, no. 3, pp. 1026–1032, Sep. 2012.

[11] L. Güvenç *et al.*, "Cooperative adaptive cruise control implementation of team mekar at the grand cooperative driving challenge," *IEEE Intell. Transp. Syst. Mag.*, vol. 13, no. 3, pp. 1062–1074, Sep. 2012.

[12] *Grand Cooperative Driving Challenge 2016*. Accessed: Sep. 2017. [Online]. Available: http://gcdc.net/en/

[13] C. Englund *et al.*, "The grand cooperative driving challenge 2016: Boosting the introduction of cooperative automated vehicles," *IEEE Wireless Commun.*, vol. 23, no. 4, pp. 146–152, Aug. 2016.

[14] H. H. Bengtsson, L. Chen, A. Voronov, and C. Englund, "Interaction protocol for highway platoon merge," in *Proc. IEEE 18th Int. Conf. Intell. Transp. Syst.*, Sep. 2015, pp. 1971–1976.

[15] K. Jo, J. Kim, D. Kim, C. Jang, and M. Sunwoo, "Development of autonomous car—Part I: Distributed system architecture and development process," *IEEE Trans. Ind. Electron.*, vol. 61, no. 12, pp. 7131–7140, Dec. 2014. [Online]. Available: http://dx.doi.org/10.1109/TIE.2014.2321342

[16] I. P. Alonso *et al.*, "Accurate global localization using visual odometry and digital maps on urban environments," *IEEE Trans. Intell. Transp. Syst.*, vol. 13, no. 4, pp. 1535–1545, Dec. 2012.

[17] H. B. Mitchell, *Multi-Sensor Data Fusion: An Introduction*, 1st ed. Berlin, Germany: Springer-Verlag, 2007.

[18] I. Skog and P. Handel, "In-car positioning and navigation technologies—A survey," *IEEE Trans. Intell. Transp. Syst.*, vol. 10, no. 1, pp. 4–21, Mar. 2009.

[19] P. J. Hargrave, "A tutorial introduction to Kalman filtering," in *IEE Colloquium on Kalman Filters: Introduction, Applications and Future Developments*. Harlow, U.K.: STC Technology Ltd., Feb. 1989, pp. 1–6.

[20] *06-GPS*. Accessed: Sep. 2017. [Online]. Available: http://06-gps.nl/

[21] *Intelligent Transport Systems (ITS); European Profile Standard for the Physical and Medium Access Control Layer of Intelligent Transport Systems Operating in the 5 GHz Frequency Band*, document ETSI ES 202 663 v1.1.0, 2009. [Online]. Available: http://www.etsi.org/deliver/etsi_es/202600_202699/202663/01.01.00_50/es_202663v010100m.pdf

[22] *Intelligent Transport Systems (ITS); Vehicular Communications; Geonetworking; Part 1: Requirements*, document ETSI 102 636-1 v1.1.1, 2010. [Online]. Available: http://www.etsi.org/deliver/etsi_ts/102600_102699/10263601/01.01.01_60/ts_10263601v010101p.pdf

[23] *Intelligent Transport Systems (ITS); Vehicular Communications; Geonetworking; Part 5: Transport Protocols; Sub-Part 1: Basic Transport Protocol*, document ETSI 102 636-5-1 v1.1.1, 2011. [Online]. Available: http://www.etsi.org/deliver/etsi_ts/102600_102699/1026360501/01.01.01_60/ts_1026360501v010101p.pdf

[24] *IEEE Standard for Information Technology—Local and Metropolitan area Networks—Specific Requirements—Part 11: Wireless LAN Medium Access Control (MAC) and Physical Layer (PHY) Specifications Amendment 6: Wireless Access in Vehicular Environments*, Standard 802.11p, 2010. [Online]. Available: https://www.ietf.org/mail-archive/web/its/current/pdfqf992dHy9x.pdf

[25] A. Voronov. *Voronov Code Projects on ITS-G5*. Accessed: Sep. 2017. [Online]. Available: https://github.com/alexvoronov?tab=activity

[26] *Asn1c*. Accessed: Sep. 2017. [Online]. Available: http://lionet.info/asn1c/blog/

[27] *Udp2eth*. Accessed: Sep. 2017. [Online]. Available: https://github.com/jandejongh/udp2eth

[28] D. Eckhoff, N. Sofra, and R. German, "A performance study of cooperative awareness in ETSI ITS G5 and IEEE WAVE," in *Proc. 10th Annu. Conf. Wireless Demand Netw. Syst. Services (WONS)*, Mar. 2013, pp. 196–200.

[29] G. M. Hoang, B. Denis, J. Härri, and D. T. M. Slock, "On communication aspects of particle-based cooperative positioning in GPS-aided VANETs," in *Proc. IEEE Intell. Vehicles Symp. (IV)*, Jun. 2016, pp. 20–25.

[30] D. F. Llorca *et al.*, "Autonomous pedestrian collision avoidance using a fuzzy steering controller," *IEEE Trans. Intell. Transp. Syst.*, vol. 12, no. 2, pp. 390–401, Jun. 2011.
[31] V. Milanés *et al.*, "Intelligent automatic overtaking system using vision for vehicle detection," *Expert Syst. Appl.*, vol. 39, no. 3, pp. 3362–3373, 2012. [Online]. Available: http://www.sciencedirect.com/science/article/pii/S0957417411013339

Ignacio Parra Alonso received the M.S. and Ph.D. degrees in telecommunications engineering from the University of Alcalá (UAH) in 2005 and 2010, respectively. He is currently an Assistant Professor with the Computer Engineering Department, UAH. His research interests include intelligent transportation systems, intelligent vehicles, artificial vision, and operating systems. He received the Master Thesis Award in eSafety from the ADA Lectureship at the Technical University of Madrid, Spain, in 2006, and the 3M Foundation Award under the category of eSafety in 2009.

Rubén Izquierdo Gonzalo was born in Madrid, Spain, in 1990. He received the M.Eng. degree in industrial engineering from the University of Alcalá, Alcalá de Henares, Spain. He is currently pursuing the Ph.D. degree in the improvement of trajectory planning for autonomous vehicles based on intention prediction of human-driven vehicles with the INVETT Research Group, Department of Automatics, University of Alcalá. He was in charge of the high level planning of the maneuvers in the GCDC 2016.

Javier Alonso received the European Doctor degree in computer science from the Polytechnic University of Madrid (UPM), Spain, in 2009. From 2004 to 2010, he was a Researcher with the Industrial Automation Institute, Spanish Council for Scientific Research (CSIC), where his main interest was the autonomous vehicles control. From 2010 to 2012, he was a Researcher with the Center for Automation and Robotics, UPM-CSIC, where his main interest was the cooperation among autonomous vehicles.

Álvaro García-Morcillo was born in 1993. He received the Electronics and Industrial Automatics Degree from the University of Alcalá, Alcalá de Henares, Spain, in 2015. He is currently pursuing the master's degree. Since 2014, he has been with the INVETT Research Group, Department of Automatics, University of Alcalá. His work was focused on curb and free space detection, and the implementation of the communications system for the GCDC 2016.

David Fernández-Llorca received the M.S. and Ph.D. degrees in telecommunications engineering from the University of Alcalá (UAH), Madrid, Spain, in 2003 and 2008, respectively. He is currently an Associate Professor with UAH. He has authored over 90 refereed publications in international journals, book chapters, and conference proceedings. His research interests include computer vision and intelligent transportation systems. He is currently an Associate Editor of the IEEE TRANSACTIONS ON INTELLIGENT TRANSPORTATION SYSTEMS.

Miguel Ángel Sotelo received the degree in electrical engineering from the Technical University of Madrid in 1996, the Ph.D. degree in electrical engineering from the University of Alcalá (UAH), Madrid, Spain, in 2001, and the M.B.A. degree from the European Business School in 2008. He is currently a Full Professor with the Department of Computer Engineering, UAH. He has authored 200 publications in journals, conferences, and book chapters. His research interests include real-time computer vision and control systems for autonomous and assisted intelligent road vehicles. He received the Best Research Award in the domain of Automotive and Vehicle Applications in Spain in 2002 and 2009, the IEEE ITSS Outstanding Application Award in 2013, and the 3M Foundation Awards in the category of eSafety in 2004 and 2009. He was a recipient of the 2010 Outstanding Editorial Service Award for the IEEE Transactions on Intelligent Transportation Systems. He has served as a Project Evaluator, a Rapporteur, and a Reviewer for the European Commission in the field of ICT for Intelligent Vehicles in FP6 and FP7. He has served as the General Chair of the 2012 IEEE Intelligent Vehicles Symposium Alcalá de Henares, Spain, in 2012. He is the Editor-in-Chief of the *IEEE Intelligent Transportation Systems Magazine*.